

# Normalised Detection of Clock States by Cold Atom Recapture Method

S. Walby<sup>1,2</sup>, M. Knapp<sup>1,2</sup>, J. Whale<sup>2</sup>, A. Wilson<sup>2</sup>, R. Hendricks<sup>2</sup>, C.J. Foot<sup>1</sup>, K. Szymaniec<sup>2</sup>

<sup>1</sup>Department of Physics, University of Oxford, Oxford, UK

<sup>2</sup>National Physical Laboratory, Teddington, UK

sam.walby@npl.co.uk

**Summary**—A method of detecting normalised clock state populations in an atomic fountain clock using only the initial trapping laser beams has been investigated. The results suggest that, after refining the design of the trapping chamber, the achievable signal-to-noise ratio will be limited by the phase noise of a quartz local oscillator. This provides a way to miniaturise an atomic fountain clock with only a small reduction in performance.

Very good long-term stability is an essential requirement for a frequency standard or a hold-over clock in a local time scale realisation. In cold atom clocks and frequency standards the absorbers do not interact with walls or a buffer gas and thus can possess an ultimate long-term stability limited only by uncontrolled time variations of major systematic effects. Present devices targeting the highest stability and accuracy at parts in  $10^{16}$ , usually large installations of cold atomic fountains, are mainly commissioned at major national measurement labs [1, 2]. More recently, smaller constructions with accuracies in the  $10^{-15}$  range have also been built and commercialised [3, 4]. One can expect a potentially sizeable market for compact cold atoms clocks with short- and long-term stability comparable to the best current primary standards.

A new project at NPL aims to develop a miniature cold atom fountain clock that, despite necessary reductions in size, weight, and power consumption, would perform at a level similar to the established ‘full size’ fountain clocks. Its short-term stability should be close to  $10^{-13}/\tau^{1/2}$ , limited mainly by the residual phase noise of a good quartz-based local oscillator; its long-term instability, dominated by temporal variations of major systematic effects, should not exceed parts in  $10^{16}$ . It should also be possible to perform a full evaluation of the systematic effects and use such a mini-fountain as a primary or secondary frequency standard. The design intends to preserve the approximately 0.5 s Ramsey interrogation time of the large fountain clocks, requiring atoms to be launched about 30 cm above the microwave cavity, so the savings on size and weight should come from reducing other parts of the physics package,

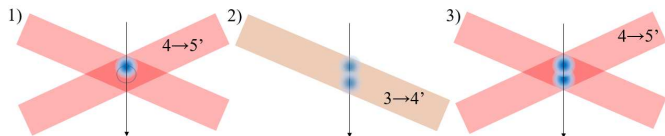


Fig. 1. Sequence for normalised detection with MOT beams. 1) First detection pulse induces fluorescence to obtain  $S_1$ . 2) Repump puts all atoms back into upper level. 3) Second detection pulse induces fluorescence to obtain  $S_2$ .

optics and auxiliary electronics.

An important step in that direction would be to eliminate the separate chamber normally used for detection of the clock state populations. This requires combining the cooling and trapping functionality with that of fluorescence detection in a single compact vacuum chamber. In this paper we present preliminary results for a detection scheme where the clock state populations are measured with a recapture method using the cooling beams. While the measurement of the upper clock state population, from which the cooling (cycling) transition is excited, is rather straightforward, the shot-to-shot fluctuations of the number of atoms collected and detected can significantly limit the achievable signal-to-noise ratio (SNR). Population normalisation procedures have been demonstrated in the past [5, 6, 7] for different experimental contexts, each with their own limitations. Here the normalisation is achieved by applying two short pulses of all six cooling beams coinciding with the atomic cloud re-entering the molasses region after the ballistic flight in the fountain (fig. 1). The first pulse induces fluorescence from the upper clock state population (here, the  $F = 4$  state in Cs) by driving the cycling  $|F\rangle \rightarrow |F + 1\rangle$  transition. A pulse of repumper light then swiftly transfers all the atoms (those originally in the lower clock state as well as those pumped to this state by off-resonant excitation of the  $|F\rangle \rightarrow |F\rangle$  transition during the first detection pulse) to the upper state, such that a second detection pulse induces fluorescence from the total number of atoms. The ratio of the integrated signals,  $S_1$  and  $S_2$ , generated by the two detection pulses, respectively, corresponds to a normalised clock transition probability  $P = S_1/S_2$  (fig. 2). For simplicity and compactness of the physics package, the atoms are initially collected from a background

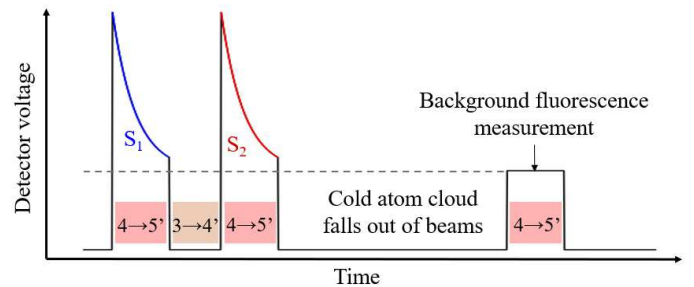


Fig. 2. Illustration of the voltage-time signal, along with the corresponding excited transitions.  $S_1$  and  $S_2$  are the areas under the blue and red curves, respectively, after subtracting the background level (dashed line).

vapour in a single stage magneto-optical trap (MOT). As a result, significant fractions of the signals  $S_1$  and  $S_2$  come from the room temperature atoms. To measure and subtract this contribution a third pulse is applied at the end of the detection sequence.

The technique has been tested on the NPL-CsF3 fountain (with the  $\langle 100 \rangle$  cooling geometry and a cloud temperature after the sub-Doppler cooling phase of 2  $\mu\text{K}$ ) and on a provisional demonstrator setup (with the  $\langle 111 \rangle$  geometry, cloud temperature 10  $\mu\text{K}$ ). Using the former to launch the atoms for a flight time of 600 ms (45 cm launch height), the returning atom number was varied by varying the initial MOT loading time from between 0.1 s and 2.0 s. Measuring the SNR as a function of detected atom number,  $N_{\text{at}}$ , yields information on what is limiting it:

$$\text{SNR} = \frac{N_{\text{at}}}{\sqrt{\sigma_{\text{const}}^2 + \sigma_{\text{QPN}}^2 N_{\text{at}} + (\sigma_{\text{prop}} N_{\text{at}})^2}} \quad (1)$$

where  $\sigma_{\text{const}}$  is constant noise, such as electrical noise in the detection system, that is suppressed with a larger detected signal,  $\sigma_{\text{QPN}}$  is the coefficient for the quantum-projection noise, which accounts for the atom cloud being in a coherent superposition of the upper and lower levels, and  $\sigma_{\text{prop}}$  is noise that is proportional to the cold-atom signal, and thus presents a high- $N_{\text{at}}$  limit to the SNR. Since neither the provisional demonstrator system, nor CsF3 at this reduced launch height, made use of a microwave cavity for interrogation, the atomic cloud is purely in the upper state, and  $\sigma_{\text{QPN}} = 0$ . A plot of SNR vs  $N_{\text{at}}$  is presented in fig. 3.

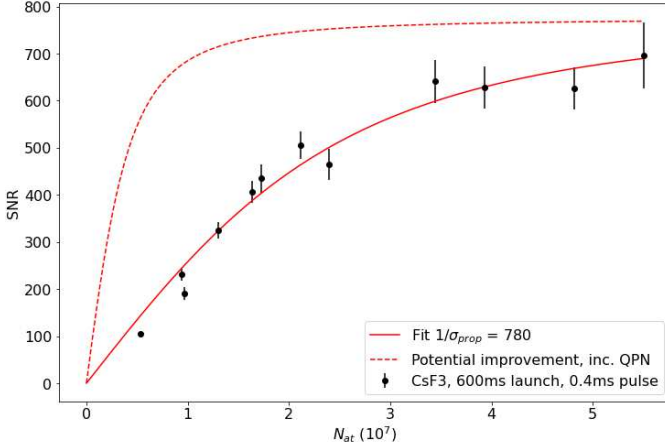


Fig.3. SNR vs  $N_{\text{at}}$  for 600 ms launches in CsF3. The solid line is the fit to the current data, the dashed line is the potential improvement due to increasing the fluorescence collection efficiency by a factor of six.

It was found that, for a typical  $N_{\text{at}} \approx 4.0 \times 10^7$ , the detection SNR was maximised, at around 700, when each of the six MOT beams had a central intensity of around 6  $\text{mW}/\text{cm}^2$  during the detection pulses. Lower intensity allows for greater fluctuation of the cold-atom fluorescence with laser intensity fluctuations (while CsF3's detection beams are intensity-stabilised, the MOT beams are not). However, because of a significant pressure of Cs background gas, which is Doppler-broadened such that the background fluorescence is far from saturation, increasing the intensity further amplifies background noise

without improving the size or stability of the cold-atom signal. Additionally, the off-resonant pumping is also far from saturation; laser intensity fluctuations affect the decay rate and thus the total cold-atom signal. The optimum detuning of the MOT beams during detection was found to be  $\delta = -1.8 \Gamma$ . The length of each detection pulse was adjusted to optimise the SNR, and an optimum was found for 0.4 ms detection pulses, separated by a repump pulse of 0.1 ms. The exact timings of the background pulse did not appreciably affect the measured SNR, although care was taken to allow the entire cloud to pass out of the beam region before performing the background measurement.

Further increasing the atom number did not increase the SNR when detecting the entire cloud; fitting equation 1 to the data implies that the high-signal limit to the SNR would be 780. However, for actual fountain operation, only the  $m_F = 0$  clock state would undergo the Ramsey interrogation and be detected, which requires a state-selection method to separate the  $m_F = 0$  population from the rest of the cloud. In a Cs fountain without optical pumping to the clock state, this reduces the returning atom number by a factor of 9, which would reduce the SNR to a level where electrical noise dominates. In this case, loading more atoms would be beneficial for improving the detection SNR, however if this is achieved by spending longer loading the MOT, the dead-time in the fountain sequence is increased which increases the local-oscillator noise [8]. This motivates using  $^{87}\text{Rb}$  instead of Cs, as there would only be 5 (or 3 in the lower-level) Zeeman substates to split the atomic population between. However, further improvement to the SNR would still be required: for the detection SNR to be comparable or better than the SNR due to the phase noise of a quartz local-oscillator, it should exceed 500. Two straightforward ways to improve the low-signal SNR are to use lower-noise electronics for detection, and to increase the fluorescence collection efficiency of the detection system.

A background magnetic field of 1.9  $\mu\text{T}$  exists in CsF3's MOT chamber, which results in a frequency splitting between each of the  $|4, m_F\rangle \rightarrow |3, m_F\rangle$  microwave transitions of 6.8 kHz that was leveraged to perform state selection. A microwave horn directed into the MOT chamber was used to apply a  $\pi$ -pulse resonant with the  $|4, 0\rangle \rightarrow |3, 0\rangle$  clock transition immediately after the end of the sub-Doppler cooling phase, such that the atoms remaining in the upper state could then be pushed out of the cloud by a short, resonant pulse from the downward-going MOT beam while the cloud was still in the beam region. Thus, state selection was implemented using only the MOT beams and a microwave horn, removing the need for a separate state-selection cavity between the MOT chamber and Ramsey cavity.

A complete physics package prototype to test the short- and long-term stability is currently being designed. It would feature a small cooling chamber in the  $\langle 110 \rangle$  geometry, such that one pair of MOT beams are horizontal and the other two are at  $45^\circ$  to the vertical. The MOT loading rate depends on the fourth power of the beam diameter, so preserving the MOT beam diameter, despite otherwise minaturising the system, is important for loading a sufficient number of atoms quickly.

Such a chamber will be  $\sim 8$  cm in diameter and preserve the 24 mm beam diameter, while improving the collection efficiency to 6 % (up from 1 % for both of the present systems). This will suppress the constant technical noise by a factor of six relative to the present data. The potential result of this is illustrated by the dashed line in fig. 3. Taking into account the quantum projection noise based on the current atom number estimates, the resulting SNR for  $1/5^{\text{th}}$  of the typical signal would be 650. The Ramsey cavity will be directly vacuum-sealed to the MOT chamber, and a compact all-in-fibre optics and laser delivery system is being developed, with the aim to improve the long-term intensity stability of the MOT beams.

## REFERENCES

- [1] “BIPM Annual report on Time Activities”, Bureau International des Poids et Mesures, [https://webtai.bipm.org/ftp/pub/tai/annual-reports/bipm-annual-report/annual\\_report\\_2020.pdf](https://webtai.bipm.org/ftp/pub/tai/annual-reports/bipm-annual-report/annual_report_2020.pdf)
- [2] R. J. Hendricks, F. Ozimek, K. Szymaniec, B. Nagorny, P. Dunst, J. Nawrocki, S. Beattie, B. Jian, and K. Gibble, “Cs fountain clocks for commercial realizations – an improved and robust design”, IEEE Trans. on UFFC, vol. 66, pp. 624-631, 2019.
- [3] M. Langlois, L. De Sarlo, D. Holleville, N. Dimarcq, J.F. Schaff, and S. Bernon, “Compact cold-atom clock for onboard timebase: tests in reduced gravity”, Phys. Rev. Applied, vol. 10, 064007, 2018.
- [4] F.G. Ascarrunz, Y.O. Dudin, M.C. Delgado Aramburo, L.I. Ascarrunz, J. Savory, A. Banducci, and S. R. Jefferts, “A portable cold  $^{87}\text{Rb}$  atomic clock with frequency instability at one day in the  $10^{-15}$  range,” 2018 IEEE Int. Freq. Control Symp., 2018, pp. 1-3.
- [5] A. Clairon, P. Laurent, G. Santarelli, S. Ghezali, S. N. Lea, and M. Bahoura, “A cesium fountain frequency standard: preliminary results”, IEEE Trans. on Instr. and Meas., vol. 44, pp. 128-131, 1995.
- [6] G. W. Biedermann, X. Wu, L. Deslauriers, K. Takase, and M. A. Kasevich, “Low-noise simultaneous fluorescence detection of two atomic states”, Opt. Lett., vol. 34, pp. 347-349, 2009.
- [7] H. Song, J. Zhong, X. Chen, L. Zhu, Y. Wang, J. Wang, and M. Zhan, “Normalized detection by using the blow-away signal in cold atom interferometry”, Opt. Express, vol. 24, 28392-28399, 2016.
- [8] G. Santarelli, C. Audoin, A. Makdissi, P. Laurent, G. J. Dick and A. Clairon, “Frequency stability degradation of an oscillator slaved to a periodically interrogated atomic resonator,” in IEEE Trans. on UFFC, vol. 45, pp. 887-894, 1998.